Eur. Phys. J. C 25, 453–458 (2002)
Digital Object Identifier (DOI) 10.1007/s10052-002-1024-9

THE EUROPEAN PHYSICAL JOURNAL C

Compressible bag model and the phase structure

S. Kagiyama[1,a], S. Kumamoto[1,b], A. Minaka[2,c], A. Nakamura[1,d], K. Ohkura[1,e], S. Yamaguchi[1,f]

[1] Department of Physics, Faculty of Science, Kagoshima University, Kagoshima 890-0065, Japan
[2] Department of Physics, Faculty of Education, Kagoshima University, Kagoshima 890-0065, Japan

Received: 22 February 2002 / Revised version: 28 June 2002 /
Published online: 20 September 2002 –

Abstract. The phase structure of hadrons and the quark–gluon plasma is investigated by two types of equation of state of the hadrons, namely the ideal hadron gas model and the compressible bag model. It is pointed out that, while the ideal gas model produces an unrealistic extra hadron phase, the compressible bag model gives the expected and reasonable phase diagram even if the rich hadron spectrum is taken into account.

1 Introduction

The quark–gluon plasma (QGP) has been expected to appear at high temperature and/or high density, due to asymptotic freedom of QCD. Indeed, not a few of the experimental results up to CERN SPS incident energies suggest the existence of the QGP phase [1], and the recent experiment at BNL RHIC may give us cleaner and richer signals [2].

Theoretically, in lattice QCD calculations [3–7], no phase transition is observed for the two light, or two light and one medium light flavor cases at zero baryon density. In both cases only a continuous cross-over is observed for realistic quark mass values.

On the other hand, in a more phenomenological approach, the equations of state of QGP and hadrons are assumed, and the transition point is determined by the Gibbs condition. In this approach, the cross-over cannot be reproduced, and that may give rise to doubt on its validity. However, the authors believe that the gross structure of the phase diagram obtained in this approach should still remain valid far away from the cross-over region. It should also be noted that at a finite baryon chemical potential, not much is known from lattice QCD because of a well-known technical difficulty which makes the Monte Carlo technique inapplicable.

The purpose of the present paper is to investigate what type of equation of state of the hadrons is preferable in the phenomenological approach, where the discussion is devoted exclusively to the gross phase structure of hadrons and QGP, neglecting the multi-quark states. This means that the detailed structure around the phase transition or cross-over region is neglected.

In the phenomenological approach, there are the following problems concerning the gross structure of phase diagrams. When a simple ideal gas of nucleons is used for the equation of state of the hadrons and the MIT bag model is used for the equation of state for QGP, the hadron phase appears at high density and at zero temperature (see, e.g., [8]). This is because

$$p_h^0/p_q^0 \to 27 \quad \text{as} \quad \mu_{\rm B} \to \infty \quad (T=0), \tag{1}$$

where p_h^0 and p_q^0 denote the pressures of the ideal nucleon phase and (ideal) quark phase, respectively, and $\mu_{\rm B}$ is the baryochemical potential. To circumvent this difficulty, volume exclusion effects of hadrons of van der Waals type were taken into account (see, e.g. [8,9]; see also [10]). However, the treatments in [8–10] are thermodynamically inconsistent [11], for example, $n \neq (\partial p/\partial\mu)_T$, $s \neq (\partial p/\partial T)_\mu$. Although the formulation in [11] is thermodynamically consistent, it has still the difficulty that the pressure diverges as $n \to 1/v_0$, where n is the number density and v_0 is the fixed hadron volume, and acausality emerges (there is no relativistic rigid body) as the authors themselves pointed out. Thus we were led to the "soft core" model; that is, the compressible bag model [12,13].

In addition to the difficulty that the hadron phase appears at high density and at zero temperature, the equation of a simple ideal gas of hadrons again suffers from the same difficulty at another region; that is, at high temperature and zero baryon number density [14]. The argument in [14] is simple. At $\mu_{\rm B} = 0$ and in the high-temperature region, the pressure p_q of the QGP phase and the pressure p_h of the hadron phase are given by

$$p_q = g_q(1/90\pi^2)T^4 - B, \quad p_h = g_h(1/90\pi^2)T^4, \tag{2}$$

where g_q and g_h are the degeneracy factors in each phase, and B is the bag constant. When we consider a mixed gas

[a] e-mail: kagiyama@sci.kagoshima-u.ac.jp
[b] e-mail: kumamoto@cosmos01.cla.kagoshima-u.ac.jp
[c] e-mail: minaka@edu.kagoshima-u.ac.jp
[d] e-mail: nakamura@sci.kagoshima-u.ac.jp
[e] e-mail: ohkura@cosmos01.cla.kagoshima-u.ac.jp
[f] e-mail: yamaguchi@cosmos01.cla.kagoshima-u.ac.jp

of lower lying nonstrange hadrons, that is, π, ρ, N and Δ, the degeneracy factor g_h becomes $3+9+(7/4)(4+16) = 47$ and this exceeds $g_q = 2{\cdot}8+(7/4)4{\cdot}3 = 37$. Thus the hadron phase appears again. In the compressible bag model, however, the effective degeneracy factor of the hadron phase is greatly reduced so that the QGP phase is realized at high temperature even if infinitely many nonstrange mesons are taken into account [15].

The authors of [12,13,15] suggested that the compressible bag model gives a phase diagram free from the above difficulties, but it has not been shown explicitly. In [12] the equations of state only at $T = 0$ are used for discussing neutron stars, and in [15] are used those at $\mu_{\rm B} = 0$ for multiple production in heavy ion collisions. In [13] the phase diagram with finite T and $\mu_{\rm B}$ is calculated, but the rich hadron spectrum is neglected.

The unique purpose of the present paper is, then, to show that the compressible bag model indeed gives the naively expected phase diagram in all regions. As far as the authors know, this is the only model that satisfies the following:

(1) It is built in a thermodynamically consistent formalism.

(2) It is valid in very high-temperature regions even if rich hadron spectra are taken into account.

(3) It is explicitly calculable in whole regions, and it gives a well-behaved phase diagrams, i.e. there is no extra hadron phase.

Since the hadron level structure affects the phase diagram, we consider the following two models:

Model I: The hadron phase consists of the $N\bar{N}\pi$ system while the QGP phase consists of nonstrange quarks, their anti-quarks and gluons.

Model II: The hadron phase consists of a system of 102 species of hadrons of which the masses are less than 10.6 GeV, except for hadrons with a top quark [16]. The QGP phase consists of u-, d-, s-, c-, and b-quarks, and their anti-quarks and gluons.

Model I is a model with a few hadrons, while model II is an example which includes many hadrons.

While in [15] the continuous level-density function of [17] is used, in this paper the phase diagrams are calculated with a real spectrum of hadrons in order to avoid the model dependence. The effect of the cutoff in the hadron spectrum in model II is discussed in the final section.

In Sect. 2, for comparison the phase structure in a free point-like model is shown with the above two types of models, where one can explicitly see the difficulties explained in this section. In Sect. 3, the equation of state in the compressible bag model [13,15] is briefly reviewed, and with the resulting phase diagram it is shown that the difficulty is indeed removed. The final section is devoted to concluding remarks.

2 A difficulty in the phase structure for models of free point-like hadrons

In this section, we assume that all hadrons, quarks, and gluons are free point-like objects and discuss their phase structure. For this purpose, we present expressions for the pressures of free point-like particles in order to establish our notation in the first subsection. On the basis of these expressions, the phase diagram is discussed and a difficulty is pointed out in the second subsection.

2.1 Pressures for hadron gas and QGP

The total pressure p of a mixed gas of N species of free point-like particles is given by

$$p(T,\mu_{\rm B}) = \sum_{n=1}^{N} p_n(T,\mu_n), \tag{3}$$

where T ($\mu_{\rm B}$) is the temperature (baryochemical potential) of the gas and p_n (μ_n) is the pressure (baryochemical potential) of the nth species of particles. The pressure p_n is given by

$$p_n = \eta_n g_n T \int \frac{{\rm d}^3\boldsymbol{k}}{(2\pi)^3} \log\left[1+\eta_n \exp\left(-\frac{E_n-\mu_n}{T}\right)\right], \tag{4}$$

$$E_n = \sqrt{\boldsymbol{k}^2+m_n^2}, \tag{5}$$

$$\mu_n = a_n \mu_{\rm B}, \tag{6}$$

where η_n is a statistical factor that takes the value -1 for bosons and $+1$ for fermions, respectively. The quantities g_n, a_n, and m_n denote the degeneracy factor, the baryon number, and the mass of the nth species of particles, respectively.

In low temperature region, p_n is expanded as follows:

$$\begin{aligned} p_n = {} & \frac{g_n}{24\pi^2}\left[\mu_n k_{n{\rm F}}^3 - \frac{3}{2}m_n^2\mu_n k_{n{\rm F}} \right. \\ & \left. + \frac{3}{2}m_n^4 \log\left(\frac{\mu_n+k_{n{\rm F}}}{m_n}\right)\right] + \frac{g_n}{12}\mu_n k_{n{\rm F}} T^2 \\ & + \frac{7\pi^2 g_n}{720}\left[\frac{3\mu_n}{k_{n{\rm F}}} - \left(\frac{\mu_n}{k_{n{\rm F}}}\right)^3\right] T^4, \end{aligned} \tag{7}$$

$$k_{n{\rm F}} = \sqrt{\mu_n^2 - m_n^2}, \tag{8}$$

when the nth species of particles are fermions. In the above $k_{n{\rm F}}$ is the Fermi momentum. Equation (7) is applicable for $\mu_n > m_n$. Otherwise the pressure p_n vanishes identically.

Now let us present expressions for the pressures of hadrons and QGP. For the total pressure p_h of a mixed gas of N species of free point-like hadrons, it is given by

$$p_h(T,\mu_{\rm B}) = \sum_{i=1}^{N} p_{h_i}(T,\mu_i), \tag{9}$$

where p_{h_i} follows (4)–(8). In the following, we consider two cases for hadronic systems; that is, model I and model II, which are defined in the introduction.

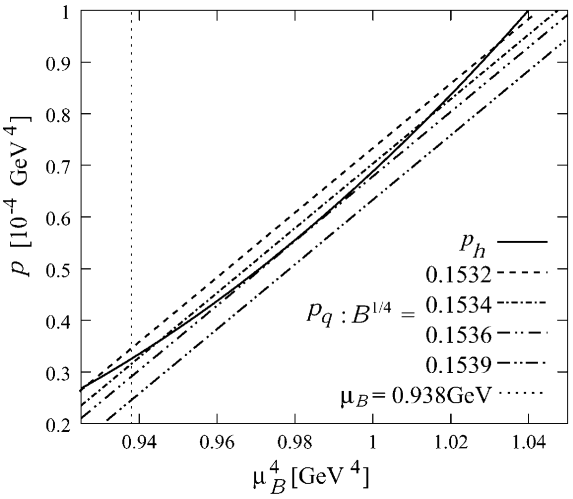

Fig. 1. p_h and p_q as functions of μ_{B}^4 for model I ($T = 0$). The unit of $B^{1/4}$ is GeV

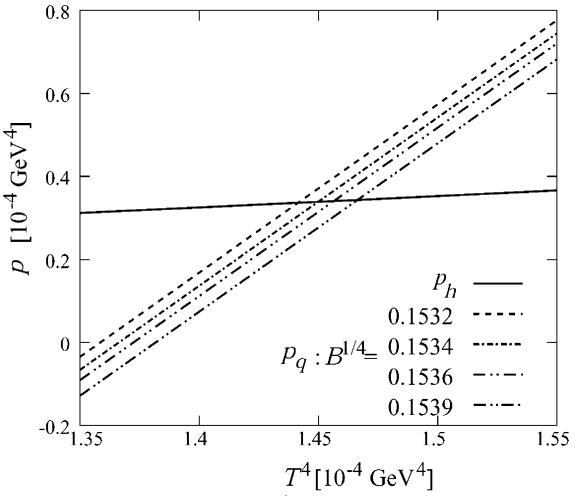

Fig. 2. p_h and p_q as functions of T^4 for the model I ($\mu_{\mathrm{B}} = 0$). The unit of $B^{1/4}$ is GeV

On the other hand, the total pressure of QGP, p_q, is given by

$$p_q(T, \mu_{\mathrm{B}}) = \sum_{j=1}^{N'} p_{q_j}(T, \mu_j) - B \tag{10}$$

in the bag model. Here p_{q_j} follows (4)–(8) and B is the bag constant. The index j denotes the species of particles, and we consider two cases, model I and model II.

2.2 Phase structure

Given the expressions of the pressures of hadron phase and QGP phase, we can consider their phase structure. The critical points are determined by the following Gibbs condition:

$$p_h(T, \mu_{\mathrm{B}}) = p_q(T, \mu_{\mathrm{B}}). \tag{11}$$

In Fig. 1, p_h and p_q are plotted as functions of μ_{B}^4, where T is fixed to zero. In Fig. 2, they are plotted as functions of T^4, where μ_{B} is fixed to zero. In both figures, calculations are performed for model I. As shown in Fig. 1, there is no critical point for $B^{1/4} > 0.1536\,\mathrm{GeV}$. For $B^{1/4} = 0.1536\,\mathrm{GeV}$, there is one critical point. For $0.1534\,\mathrm{GeV} \leq B^{1/4} < 0.1536\,\mathrm{GeV}$, there are two critical points. For $B^{1/4} < 0.1534\,\mathrm{GeV}$, there is one critical point since p_h vanishes for $\mu_{\mathrm{B}} < m_N$ and an apparent critical point in the region $\mu_{\mathrm{B}} < m_N$, where m_N is the nucleon mass, is unphysical. Therefore, at $T = 0$, an abnormal hadron phase always appears at high densities.

The reason for this difficulty is as follows. In the higher-density region of $\mu_{\mathrm{B}} \gg m_N$, the masses are negligible so that the pressures p_h and p_q are approximated as

$$p_h \approx g_h \mu_{\mathrm{B}}^4, \tag{12}$$

$$p_q \approx g_q \mu_q^4, \tag{13}$$

where g_h (g_q) is the statistical degree of freedom of the hadrons (QGP). Since $\mu_q = (1/3)\mu_{\mathrm{B}}$, (13) reads

$$p_q \approx \frac{g_q}{81} \mu_{\mathrm{B}}^4. \tag{14}$$

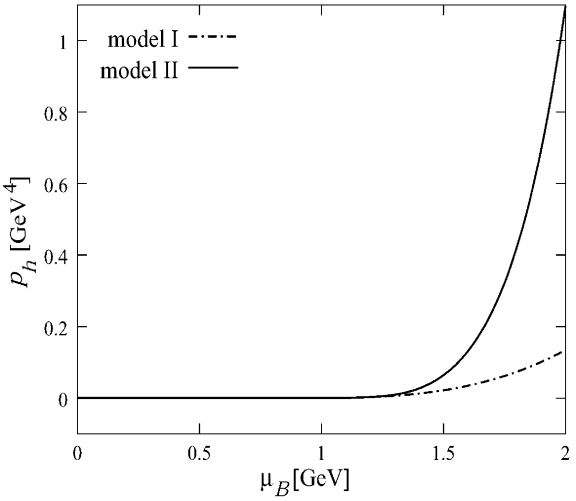

Fig. 3. p_h as functions of μ for model I and model II ($T = 0$)

Then p_h becomes large faster than p_q as μ_{B} increases, since the effective statistical degree of freedom of QGP is greatly reduced. In other words, the hadrons get a share of energy three times larger than QGP, when μ_{B} increases, so that p_h becomes larger than p_q. As a consequence the hadron phase appears in the high-density region.

Since the difficulty mentioned above stems from the qualitative nature of the model of the hadrons, and that their statistical degree of freedom is too large, we should consider to modify the model of the hadrons. So far we consider model I at present; the situation will become worse in model II, since the statistical degree of freedom further becomes large.

In Fig. 3, the p_h's for model I and model II are plotted as functions of μ_{B}, where T is fixed to zero, and in Fig. 4, p_h's for those are plotted as functions of T, where μ_{B} is fixed to zero. As seen in Fig. 3 (Fig. 4), p_h for model II becomes considerably larger than p_h for model I in the high-density (temperature) region, as expected.

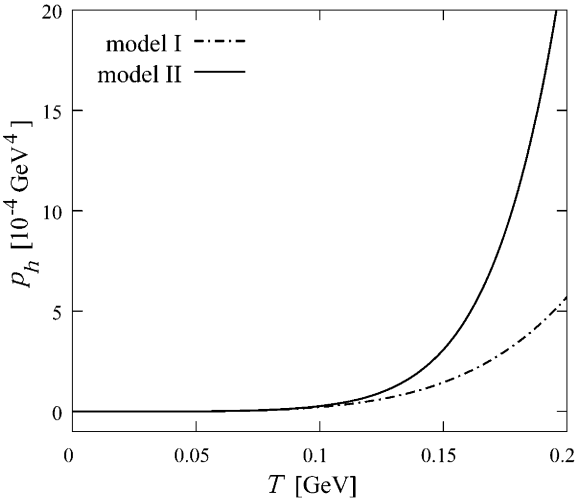

Fig. 4. p_h as functions of T for model I and model II ($\mu_{\rm B} = 0$)

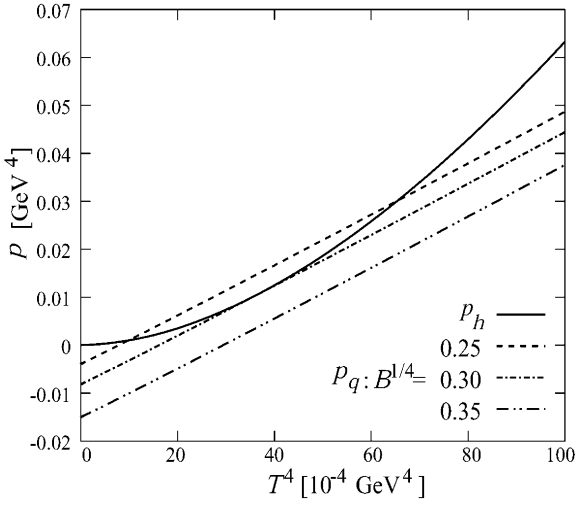

Fig. 6. p_h and p_q as functions of T^4 for model II ($\mu_{\rm B} = 0$). The unit of $B^{1/4}$ is GeV

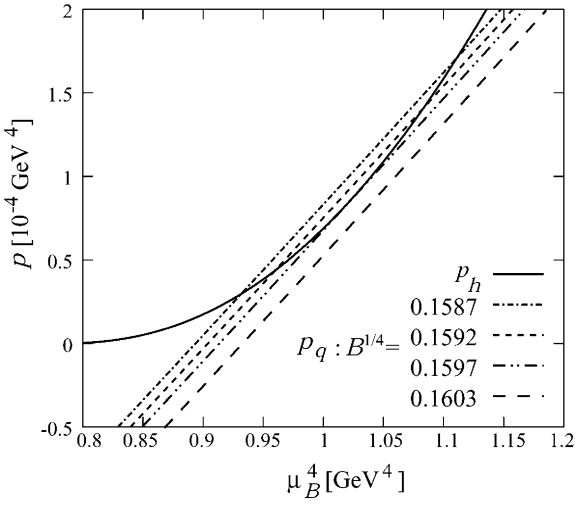

Fig. 5. p_h and p_q as functions of $\mu_{\rm B}^4$ for model II ($T = 0$). The unit of $B^{1/4}$ is GeV

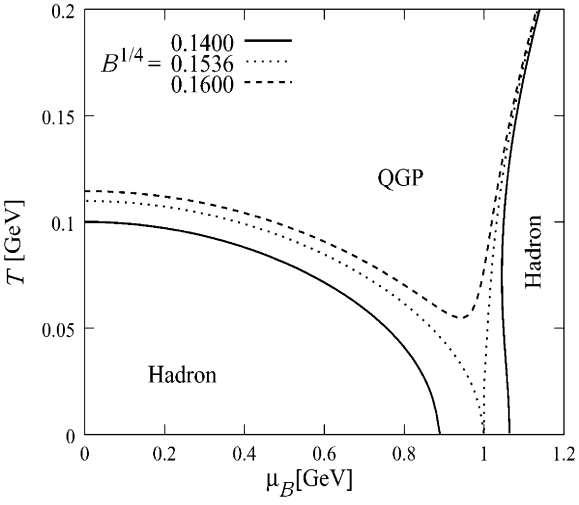

Fig. 7. Phase diagram for model I. Besides the low-density and the low-temperature region, the hadron phase appears in the high-density and low-temperature region. The unit of $B^{1/4}$ is GeV

In Fig. 5, p_h and p_q are plotted as functions of $\mu_{\rm B}^4$ with $T = 0$. In Fig. 6, they are plotted as functions of T^4 with $\mu_{\rm B} = 0$. In both figures, calculations are performed for model II. The qualitative features in Figs. 1 and 5 are the same. However, the qualitative features in Figs. 2 and 6 are different. As shown in Fig. 6, the hadron phase appears in the high-temperature region. The resulting phase diagram for model I [9] is shown in Fig. 7 and that for model II is shown in Fig. 8. The situation for model II has become worse than for model I. In order to modify this situation, we should replace the model of the hadrons with alternative ones. As one of them, we formulate the compressible bag model in the next section.

3 The compressible bag model

First, we briefly summarize the results of [13,15]. Let us suppose a mixed gas of n species of hadrons enclosed in volume V at finite temperature T. In the compressible bag model, the free energy function $\hat{F}$ of the gas is given by

$$\hat{F} = \sum_{i=1}^{n} F_{\rm f}(N_i, V', T, M_i(v_i)), \tag{15}$$

$$V' = V - b\sum_{j=1}^{n} N_j v_j, \tag{16}$$

where N_i is a number of ith species of hadrons and v_i is its volume and M_i its mass. The constant b is a volume exclusion efficiency parameter. The function $F_{\rm f}$ is the free energy function of the free point-like hadron gas. As for the mass function $M_i(v_i)$, we assume the one of the MIT bag model:

$$M_i(v_i) = A_i v_i^{-1/3} + B v_i, \tag{17}$$

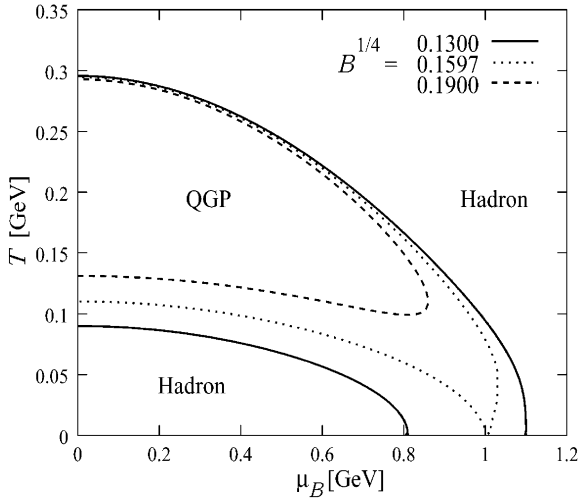

Fig. 8. Phase diagram for model II. Besides the low-density and the low-temperature region, the hadron phase appears in the high-density and the high-temperature region. The QGP phase is realized only in the mid-density and the mid-temperature region. The unit of $B^{1/4}$ is GeV

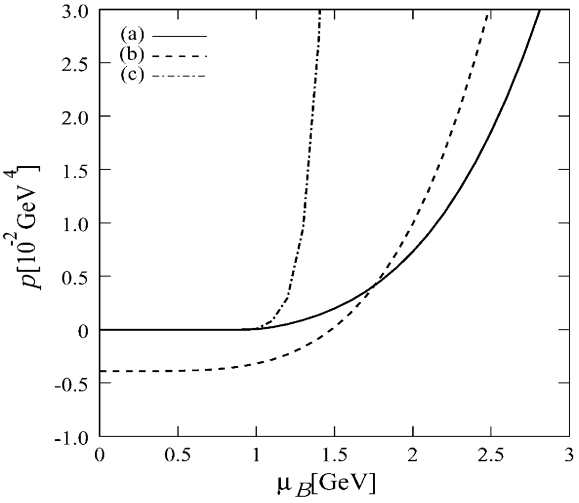

Fig. 9. (a) A solid line shows p_h as a function of μ_{B} for the compressible bag model. (b) A dashed line shows p_q for the QGP phase. (c) A dash-dotted line shows p_h for the free point-like hadron model. All lines are calculated for model II with $B^{1/4} = 0.25\,\mathrm{GeV}$ and $T = 0$

where B is the bag constant.

Under the approximation that the average of the inverse Lorentz factor of the ith species of hadrons equals unity ($\langle\gamma_i^{-1}\rangle \approx 1$) in the rest frame of the system, the basic requirement of the compressible bag model that $\partial\hat{F}/\partial v_i = 0$ and the requirement that the chemical potential of hadron should be $\mu_i = \partial\hat{F}/\partial N_i = a_i\mu_{\mathrm{B}}$, where a_i is the baryon number of the ith species of hadrons, determine the pressure p of the system as a function of T and μ_{B} by the following equation:

$$p = \sum_{i=1}^{n} \eta_i g_i T \int \frac{\mathrm{d}^3\boldsymbol{k}}{(2\pi)^3} \times \log\left\{1 + \eta_i \exp[-(E_i - \mu_i'(p, m_i))/T]\right\}, \quad (18)$$

$$E_i = \sqrt{\boldsymbol{k}^2 + M_i(p, m_i)^2},$$

$$M_i(p, m_i) = m_i \left(1 + \frac{3bp}{4B}\right)\left(1 + \frac{bp}{B}\right)^{-3/4}, \quad (19)$$

$$\mu_i'(p, m_i) = \mu_i - bv_i p = a_i\mu_{\mathrm{B}} - \frac{bm_i p}{4B}\left(1 + \frac{bp}{B}\right)^{-3/4}, \quad (20)$$

where g_i is the degeneracy factor of the ith species of hadrons and $m_i = 4(A_i/3)^{3/4}B^{1/4}$ is its mass in the vacuum.

Here two comments are in order. First p determined as above depends on b and B only in the combination of b/B since the M_i and μ_i' depend on b and B in that combination as seen in (19) and (20). Second the pressure in the compressible bag model does not become so large in the high-density and/or high-temperature region, in contrast to the one in the model of free point-like hadrons. This is because the masses of the hadrons become large in the high-density and/or high-temperature region in the compressible bag model so that the kinetic energies of the hadrons increase rather slowly and the pressure of the hadrons do not become so large. Thus the compressible bag model has a chance to evade the difficulty discussed in the previous section. In the following, we ensure that the difficulty is indeed removed, by numerical calculations.

In order to do numerical calculations, we have to fix bag constant B and the volume exclusion parameter b. The parameter b is determined by the relation

$$bv_N(p = 0) = \frac{bm_N}{4B} = \frac{4\pi}{3}(0.82\,\mathrm{fm})^3, \quad (21)$$

when the bag constant is given. The value 0.82 fm is the proton charge radius. It should be noted that the equations of state for the hadron phase are determined uniquely at this stage since the equation of states for the hadron phase only depend on b/B. We tentatively put

$$B^{1/4} = 0.25\,\mathrm{GeV}, \quad (22)$$

and then get $b = 5.0$. The resulting p_h and p_q are shown as functions of μ_{B} (T) in Fig. 9 (Fig. 10). We can recognize that the compressible bag model does not suffer from the difficulty that exists for free point-like hadrons. This point is more clearly seen by the phase diagrams shown in Fig. 11 with $B^{1/4} = 0.25\,\mathrm{GeV}$. The critical temperature T_{c} and the critical baryochemical potential μ_{c} are given by

$$T_{\mathrm{c}} = 0.18\,\mathrm{GeV}, \quad \mu_{\mathrm{c}} = 2.2\,\mathrm{GeV} \quad \text{in model I}, \quad (23)$$

$$T_{\mathrm{c}} = 0.17\,\mathrm{GeV}, \quad \mu_{\mathrm{c}} = 1.8\,\mathrm{GeV} \quad \text{in model II}. \quad (24)$$

It is noted that the equation of state of the hadrons are determined by the ratio b/B and that of QGP by B; the critical values, then, depend on B and b. If the constraint (21) is taken, the values depend only on B. As a reference, some cases are shown below:

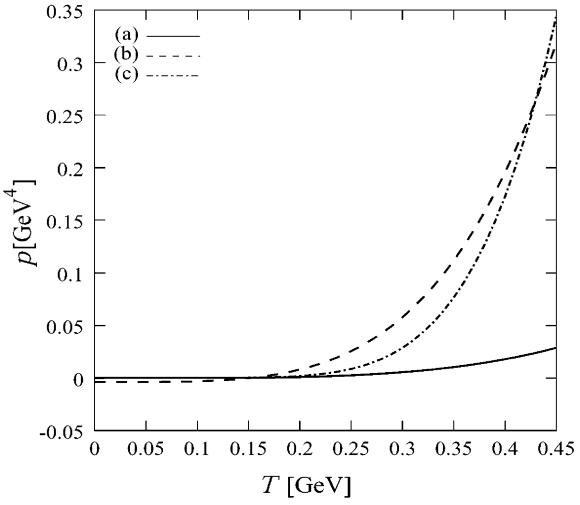

Fig. 10. (a) A solid line shows p_h as a function of T for the compressible bag model. (b) A dashed line shows p_q for the QGP phase. (c) A dash-dotted line shows p_h for the free point-like hadron model. All lines are calculated for model II with $B^{1/4} = 0.25\,\mathrm{GeV}$ and $\mu_\mathrm{B} = 0$

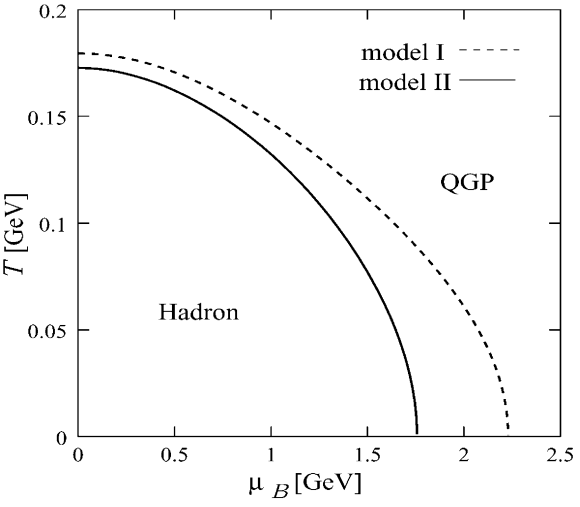

Fig. 11. Phase diagram for model II (solid line). For comparison, the phase diagram is shown for model I (dashed line). Calculations are done with $B^{1/4} = 0.25\,\mathrm{GeV}$

$$T_\mathrm{c} = 0.14\,\mathrm{GeV}, \quad \mu_\mathrm{c} = 1.7\,\mathrm{GeV} \quad \text{in model I}, \quad (25)$$
$$T_\mathrm{c} = 0.14\,\mathrm{GeV}, \quad \mu_\mathrm{c} = 1.4\,\mathrm{GeV} \quad \text{in model II}, \quad (26)$$

for $B^{1/4} = 0.20\,\mathrm{GeV}$ and

$$T_\mathrm{c} = 0.22\,\mathrm{GeV}, \quad \mu_\mathrm{c} = 2.7\,\mathrm{GeV} \quad \text{in model I}, \quad (27)$$
$$T_\mathrm{c} = 0.21\,\mathrm{GeV}, \quad \mu_\mathrm{c} = 2.1\,\mathrm{GeV} \quad \text{in model II}, \quad (28)$$

for $B^{1/4} = 0.30\,\mathrm{GeV}$.

From Figs. 9–11 one can see that the compressible bag model gives an expected and reasonable phase diagram in the whole regions. This result is stable in the sense that one can choose the bag constant from a rather wide range.

4 Concluding remarks

In this paper, it has been shown by explicit calculations that the compressible bag model gives a well-behaved phase diagram in the whole regions, even if many hadron states are taken into account. In the present calculation it is true that, even in model II, the infinite series of hadrons are cut off at finite mass, but the compressible bag model may give the expected phase diagram if an infinite series of hadrons are included. This is because, in the model, the masses of the hadrons increase and the effect of a higher mass state is much suppressed in high-temperature or high-density regions. Indeed in [15] a continuous level-density function is used for hadrons and it is shown that the abnormal hadron phase does not appear in the compressible bag model, although limited at $\mu_\mathrm{B} = 0$.

Free point-like models produce an unnatural hadron state in high-temperature or high-density regions as shown in Sects. 1 and 2. A way to avoid this difficulty is the compressible bag model, and it is worth examining it in various phenomenological analyses.

References

1. Proceedings of the International Conference on Ultra-Relativistic Nucleus–Nucleus Collisions (Quark Matter), Nucl. Phys. A **661**, (1999); **638**, (1998); **610**, (1997)
2. Proceedings of the 15th International Conference on Ultra-Relativistic Nucleus-Nucleus Collisions (Quark Matter 2001), Long Island, New York, 2001, edited by T.J. Hallman, D.E. Kharzeev, J.T. Mittcell, T. Ullrich (Elsevier, New York 2002)
3. Lattice 2000, 18th International Symposium on Lattice Field Theory, Nucl. Phys. B (Proc. Suppl.) **94**, (2001)
4. Proceedings of the International Workshop Non-Purturbative Methods and Lattice QCD (World Scientific, Singapore 2001)
5. O. Philipsen, in Lattice 2000, Nucl. Phys. Proc. Suppl. **94**, 49 (2001); hep-lat/0011019
6. F. Karsh, Lattice QCD at High Temperature and Density, hep-lat/0106019
7. Z. Foder, S.D. Katz, in Lattice 2001, Nucl. Phys. Suppl. **106**, 441 (2002); hep-lat/0110102
8. J. Cleymans, K. Redlich, H. Satz, E. Suhonen, Z. Phys. C **33**, 151 (1986)
9. H. Kouno, F. Takagi, Z. Phys. C **42**, 209 (1989)
10. R. Hagedorn, J. Rafelski, Phys. Lett. B **97**, 136 (1980)
11. D.H. Rischke, M.I. Gorenstein, H. Stöcker, W. Greiner, Z. Phys. C **51**, 485 (1991)
12. S. Kagiyama, A. Nakamura, T. Omodaka, Z. Phys. C **53**, 163 (1992); **56**, 557 (1992)
13. S. Kagiyama, A. Minaka, A. Nakamura, Prog. Theor. Phys. **95**, 793 (1996)
14. S. Kagiyama, A. Nakamura, XI International Conference on Particle and Nuclei (PANIC '87), Abstract Book II, 456
15. S. Kagiyama, A. Minaka, A. Nakamura, Prog. Theor. Phys. **89**, 1227 (1993)
16. Particle Data Group, Eur. Phys. J. C **19**, 1 (2000)
17. J.I. Kapusta, Phys. Rev. D **23**, 2444 (1981)